

Set-membership versions of improved normalized subband adaptive filter algorithm for highly noisy system

Yi Yu • Haiquan Zhao • Badong Chen

Abstract. In order to improve the performances of the recently-presented improved normalized subband adaptive filter (INSAF) algorithm for highly noisy system, this paper proposes a set-membership version of the INSAF algorithm (SM-INSAF) by exploiting the concept of the set-membership filtering. Apart from obtaining lower steady-state error under the same convergence rate, the proposed algorithm significantly reduces the overall computational complexity. In addition, to further reduce the steady-state error of the SM-INSAF, its smooth variant is developed by using smooth subband output errors to update the step sizes, called the SSM-INSAF algorithm. Simulation results in low signal-noise-ratio (SNR) environments, demonstrate the superiority of the proposed algorithms.

Keywords. Improved normalized subband adaptive filter • low SNR • set-membership filtering • smooth filtering

1 Introduction

As a subfield of signal processing techniques, adaptive filter has obtained numerous applications such as system identification, echo cancellation, channel equalization, and channel estimation [1, 2]. Owing to its simplicity and ease of implementation, the normalized least mean square (NLMS) algorithm attracts much attention. So far, a large number of NLMS-variants were proposed from different criteria to further improve its performance [3-6]. However, this class of algorithms exist a common problem that is slow convergence when the input signals are colored, especially for speech input signal.

Aiming to such input signals, an attractive approach is to use the subband adaptive filter (SAF) [2, 10]. In the SAF, the colored input signal is divided into almost mutually exclusive multiple subband signals and each subband signal is

Y. Yu • H. Zhao (✉)
School of Electrical Engineering, Southwest Jiaotong University, Chengdu, China
e-mail: hqzhao@home.swjtu.edu.cn

Y. Yu
e-mail: yuyi_xyuan@163.com

B. Chen
School of Electronic and Information Engineering, Xi'an Jiaotong University, Xi'an, China.
e-mail: chenbd@mail.xjtu.edu.cn

approximately white, thereby improving the convergence rate. For the colored input signals, the family of affine projection (AP) algorithms (see [7-9] and the references therein) can also speed up convergence because of their decorrelating property in the time-domain. Unfortunately, they also require very large computational complexity, due mainly to involving the matrix inversion operation in the update of the tap-weight vector. In [11], Lee and Gan proposed a normalized SAF (NSAF) algorithm based on the principle of the minimum disturbance. As compared to the NLMS, the NSAF provides faster convergence rate for the colored input signals. Also, this algorithm retains almost the same computational complexity as the NLMS, especially for applications of long adaptive filter such as echo cancellation. Following this algorithm, many works from the following aspects have been reported to obtain its improvement in the performances (including the convergence rate, steady-state error and computational complexity) [12-16]. In [12] and [13], to overcome a tradeoff between the convergence rate and steady-state error, two variable step size NSAF algorithms were proposed, with increased computational burden. On the other hand, to reduce the final estimation error of the NSAF when identifying a highly noisy system (or low signal-noise-ratio (SNR) system), an improved version (INSAF) [14, 15] was proposed by reusing past tap-weight vectors at each iteration, also with a moderate increase in the computational cost. However, it is desired that efforts make sense in pursuing fast convergence rate, low steady-state error and low computational complexity at the same time. Interestingly, the set-membership (SM) adaptive filter attempts to implement these three properties [6, 7, 16-18]. The fundamental idea is that the tap-weight vector is updated only when the magnitude of the estimated error exceeds a predetermined bound. Recently, the set-membership NSAF (SM-NSAF) algorithm was proposed in [16], which outperforms the NSAF in these three properties.

In this paper, the concept of the SM filtering is introduced into the INSAF, and the resulting SM-INSAF algorithm achieves low steady-state error as well as computational complexity. Subsequently, a smooth SM-INSAF (SSM-INSAF) algorithm is proposed to further reduce the steady-state error.

2 Review the INSAF

Consider a desired signal $d(n)$ that originates from an unknown system

$$d(n) = \mathbf{u}^T(n) \mathbf{w}_o + \eta(n), \quad (1)$$

where $(\bullet)^T$ indicates the transpose of a vector or matrix, \mathbf{w}_o is the unknown M -dimensional vector that we want to estimate, $\mathbf{u}(n) = [u(n), u(n-1), \dots, u(n-M+1)]^T$ is the input signal vector, and $\eta(n)$ indicates a zero-mean system noise. Fig. 1 shows the block diagram of multiband-structured SAF, where $\mathbf{w}(k) = [w_1(k), w_2(k), \dots, w_M(k)]^T$ denotes the tap-weight vector of adaptive filter that is also the estimate of \mathbf{w}_o at time index k , and N denotes number of subbands. The desired signal $d(n)$ and input signal $u(n)$ are divided into

multiple subband signals $d_i(n)$ and $u_i(n)$, respectively, through the analysis filter bank $\{H_i(z), i \in [0, N-1]\}$. Here, n indicates the time index in the original sequences. Then, the subband signals $y_{i,D}(k)$ and $d_{i,D}(k)$ are generated by critically decimating $y_i(n)$ and $d_i(n)$, respectively. It is easy to know that the i th subband error signal is given by

$$e_{i,D}(k) = d_{i,D}(k) - y_{i,D}(k) = d_{i,D}(k) - \mathbf{u}_i^T(k) \mathbf{w}(k) \quad (2)$$

where $\mathbf{u}_i(k) = [u_i(kN), u_i(kN-1), \dots, u_i(kN-M+1)]^T$, and $d_{i,D}(k) = d_i(kN)$.

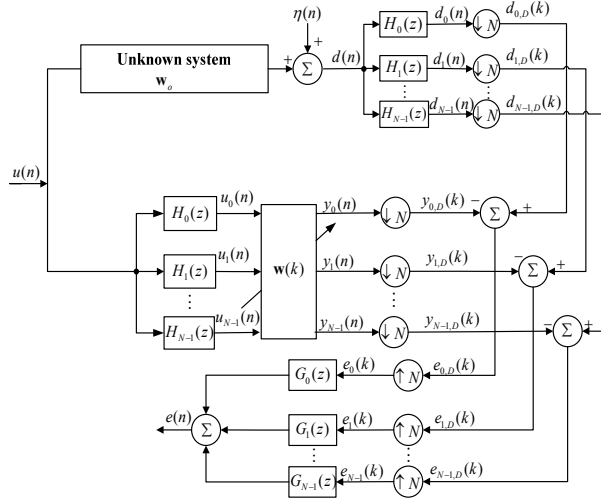


Fig. 1. Block diagram of multiband-structured SAF.

As described in [15], the original INSAF algorithm is expressed as

$$\mathbf{w}(k+1) = \frac{1}{P} \sum_{L=0}^{P-1} \mathbf{w}(k-L) + \mu \sum_{i=0}^{N-1} \frac{\xi_{i,D}(k) \mathbf{u}_i(k)}{\|\mathbf{u}_i(k)\|^2} \quad (3)$$

where μ is the step-size, P denotes the number of using past tap-weight vectors, $\|\cdot\|$ denotes l_2 -norm of a vector, and

$$\xi_{i,D}(k) = d_{i,D}(k) - \mathbf{u}_i^T(k) \frac{1}{P} \sum_{L=0}^{P-1} \mathbf{w}(k-L). \quad (4)$$

3 Proposed set-membership algorithms

3.1 Derivation of SM-INSAF

Define the subband input matrix and subband desired signal vector as follows:

$$\mathbf{U}(k) = [\mathbf{u}_0(k), \mathbf{u}_1(k), \dots, \mathbf{u}_{N-1}(k)] \quad (5)$$

$$\mathbf{d}_D(k) = [d_{0,D}(k), d_{1,D}(k), \dots, d_{N-1,D}(k)]. \quad (6)$$

To derive the SM-INSAF algorithm, we define a new constrained optimization criterion as

$$\min_{\mathbf{w}^{(k+1)}} \left\{ \sum_{L=0}^{P-1} \rho^L \|\mathbf{w}(k+1) - \mathbf{w}(k-L)\|^2 \right\} \quad (7)$$

subject to

$$\mathbf{d}_D(k) - \mathbf{U}^T(k)\mathbf{w}(k+1) = \mathbf{g}(k) \quad (8)$$

where $0 < \rho \leq 1$ is the forgetting factor, and $\mathbf{g}(k) \triangleq [g_0(k), g_1(k), \dots, g_{N-1}(k)]^T$ is the subband error-bound vector.

According to the method of Lagrange multipliers, we get

$$f(k) = \sum_{L=0}^{P-1} \rho^L \|\mathbf{w}(k+1) - \mathbf{w}(k-L)\|^2 + [\mathbf{d}_D(k) - \mathbf{U}^T(k)\mathbf{w}(k+1) - \mathbf{g}(k)]^T \boldsymbol{\theta} \quad (9)$$

where $\boldsymbol{\theta} = [\theta_1, \theta_2, \dots, \theta_N]^T$ is the Lagrange multiplier vector.

Let the derivative of (9) with respect to $\mathbf{w}(k+1)$ equal to zero, we have

$$\mathbf{w}(k+1) = \alpha \sum_{L=0}^{P-1} \rho^L \mathbf{w}(k-L) + \frac{1}{2} \alpha \mathbf{U}(k) \boldsymbol{\theta} \quad (10)$$

where $\alpha \triangleq \left(\sum_{L=0}^{P-1} \rho^L \right)^{-1}$. Substituting (10) into (8) yields

$$\boldsymbol{\theta} = 2\alpha^{-1} \left(\mathbf{U}^T(k)\mathbf{U}(k) \right)^{-1} (\boldsymbol{\varepsilon}_D(k) - \mathbf{g}(k)) \quad (11)$$

where

$$\boldsymbol{\varepsilon}_D(k) = \mathbf{d}_D(k) - \alpha \mathbf{U}^T(k) \sum_{L=0}^{P-1} \rho^L \mathbf{w}(k-L). \quad (12)$$

Combining (10) and (11), we obtain

$$\mathbf{w}(k+1) = \alpha \sum_{L=0}^{P-1} \rho^L \mathbf{w}(k-L) + \mathbf{U}(k) \left(\mathbf{U}^T(k)\mathbf{U}(k) \right)^{-1} (\boldsymbol{\varepsilon}_D(k) - \mathbf{g}(k)). \quad (13)$$

Using the assumption that the off-diagonal components of the matrix $\mathbf{U}^T(k)\mathbf{U}(k)$ can be neglected [11], (13) is simplified as

$$\mathbf{w}(k+1) = \bar{\mathbf{w}}(k) + \mu \sum_{i=0}^{N-1} \frac{(\varepsilon_{i,D}(k) - g_i(k)) \mathbf{u}_i(k)}{\|\mathbf{u}_i(k)\|^2} \quad (14)$$

where $\bar{\mathbf{w}}(k) = \alpha \sum_{L=0}^{P-1} \rho^L \mathbf{w}(k-L)$ denotes the average of the recent P tap-weight vectors, and $\varepsilon_{i,D}(k)$ is the i th element of $\boldsymbol{\varepsilon}_D(k)$, i.e.,

$$\varepsilon_{i,D}(k) = d_{i,D}(k) - \mathbf{u}_i^T(k) \bar{\mathbf{w}}(k). \quad (15)$$

Based on the SM filtering theory [6, 7, 16], we assume if the average tap-weight vector $\bar{\mathbf{w}}(k)$ lies in the constraint set H_k at k th iteration defined by

$$\mathbf{H}_k = \left\{ \bar{\mathbf{w}} : \left| d_{i,D}(k) - \mathbf{u}_i^T(k) \bar{\mathbf{w}} \right| \leq \gamma, i \in [0, N-1] \right\}, \quad (16)$$

then adaptive filter will stop updating and adaptive solution is obtained, where γ is a prespecified boundary of the constraint set \mathbf{H}_k related to the subband errors. In other words, the adaptive filter only works in the condition of $|\varepsilon_{i,D}(k)| > \gamma$. Hence, (14) can be changed as

$$\mathbf{w}(k+1) = \begin{cases} \bar{\mathbf{w}}(k) + \mu \sum_{i=0}^{N-1} \frac{(\varepsilon_{i,D}(k) - g_i(k)) \mathbf{u}_i(k)}{\|\mathbf{u}_i(k)\|^2}, & \text{if } |\varepsilon_{i,D}(k)| > \gamma \\ \bar{\mathbf{w}}(k), & \text{otherwise} \end{cases}. \quad (17)$$

Next, an important problem is how to choose the subband error-bounds $g_i(k)$ for $i \in [0, N-1]$. It has been reported in [7] that the only condition of choosing $g_i(k)$ is $|g_i(k)| \leq \gamma$. Evidently, for such a condition, there are an infinite number of ways for choosing $g_i(k)$, and each one will lead to a different algorithm. However, a widely used way is to choose $g_i(k) = \gamma \text{sgn}(\varepsilon_{i,D}(k))$ [7, 16], so that the adaptive solution locates at the nearest boundary of \mathbf{H}_k , where $\text{sgn}(\bullet)$ indicates the sign function. Applying this method into (17), the SM-INSFAF algorithm for updating the tap-weight vector is expressed as

$$\mathbf{w}(k+1) = \bar{\mathbf{w}}(k) + \sum_{i=0}^{N-1} \frac{\mu_i(k) \varepsilon_{i,D}(k) \mathbf{u}_i(k)}{\|\mathbf{u}_i(k)\|^2} \quad (18)$$

where

$$\mu_i(k) = \begin{cases} 1 - \frac{\gamma}{|\varepsilon_{i,D}(k)|}, & \text{if } |\varepsilon_{i,D}(k)| > \gamma \\ 0, & \text{otherwise} \end{cases}. \quad (19)$$

Note that, in the case of $\rho = 1$, the SM-INSFAF algorithm simply becomes

$$\mathbf{w}(k+1) = \frac{1}{P} \sum_{L=0}^{P-1} \mathbf{w}(k-L) + \sum_{i=0}^{N-1} \frac{\mu_i(k) \varepsilon_{i,D}(k) \mathbf{u}_i(k)}{\|\mathbf{u}_i(k)\|^2} \quad (20)$$

where

$$\varepsilon_{i,D}(k) = \xi_{i,D}(k) = d_{i,D}(k) - \mathbf{u}_i^T(k) \frac{1}{P} \sum_{L=0}^{P-1} \mathbf{w}(k-L). \quad (21)$$

3.2 Derivation of SSM-INSFAF

To further improve the performance of the SM-INSFAF in the steady-state, the subband error signals $\varepsilon_{i,D}(k)$, $i \in [0, N-1]$ in (19) are replaced with their own smooth estimations $\sigma_{\varepsilon_{i,D}}(k)$, i.e.,

$$\sigma_{\varepsilon_{i,D}}(k) = \beta\sigma_{\varepsilon_{i,D}}(k-1) + (1-\beta)|\varepsilon_{i,D}(k)| \quad (22)$$

where β is a smooth factor which is chosen by $\beta = 1 - N/\kappa M$, $\kappa \geq 1$ [12]. Accordingly, (19) is changed as

$$\mu_i(k) = \begin{cases} 1 - \frac{\gamma}{\sigma_{\varepsilon_{i,D}}(k)}, & \text{if } |\varepsilon_{i,D}(k)| > \gamma \\ 0, & \text{otherwise} \end{cases}. \quad (23)$$

Iterating the use of (24), we have

$$\sigma_{\varepsilon_{i,D}}(k) = (1-\beta) \sum_{l=1}^k \beta^{k-l} |\varepsilon_{i,D}(k)|. \quad (24)$$

As can be seen, $\sigma_{\varepsilon_{i,D}}(k)$ is the output of $|\varepsilon_{i,D}(k)|$ through a low-pass filter, which eliminates the effect of the fluctuation of $|\varepsilon_{i,D}(k)|$ on $\mu_i(k)$ in (23). Therefore, the resulting SSM-INSAF algorithm can reduce the steady-state error of SM-INSAF.

3.3 Discussions

Remark 1: By observing (4) and (18), we find that both proposed SM-INSAF and SSM-INSAF algorithms can be considered as variable step size INSAF algorithms. And, each subband has an individual time-varying step size $\mu_i(k)$, as shown in (19) and/or (23). Because of this property, the proposed SM-INSAF and SSM-INSAF algorithms can fast converge and reduce the steady-state error in comparison with the INSAF. Besides, when the magnitude of the i th subband error signal, i.e., $|\varepsilon_{i,D}(k)|$, is less than the bound γ , the step size $\mu_i(k) = 0$. This means the corresponding subband does not involve the update of the tap-weight vector, thus giving rise to the reduction of the computational complexity in the overall adaptation process.

Similar to the method in [16], the bound γ can be chosen by $\gamma = \sqrt{t\sigma_\eta^2 / N}$, where σ_η^2 is the variance of the system noise. It is worth mentioning that the choice of the parameter t for both proposed algorithms must consider a tradeoff between the convergence rate, steady-state error and computational burden. Namely, a large t reduces the steady-state error and overall computational complexity of both proposed algorithms, while slows the convergence rate, vice versa. Nevertheless, based on our extensive simulations, it is found that $t \in [1, 4]$ for the SM-INSAF and $t \in [0.7, 0.9]$ for the SSM-INSAF can yield good tradeoff performances. As results, both proposed SM-INSAF and SSM-INSAF algorithms are summarized in Table 1.

Remark 2: We investigate the relations of both proposed algorithms and some existing algorithms (e.g., the NSAF, INSAF and SM-NSAF), as follows:

- 1) The SSM-INSAF is a smooth version of SM-INSAF, i.e., both algorithms are equivalent when $\beta = 0$;
- 2) If P that indicates the number of using past tap-weight vectors is equal to 1, then the SM-INSAF becomes the SM-NSAF;

- 3) If $\gamma = 0$, then the SM-INSAF is reduced to the INSAF;
- 4) If in addition $P = 1$ and $\gamma = 0$, the SM-INSAF will reduce to the NSAF.

Table 1. Summary of the SM-INSAF and SSM-INSAF algorithms

Initializations	$\mathbf{w}(0) = \mathbf{0}$ P , number of using past tap-weight vector N , number of subbands $\sigma_{\varepsilon_{i,D}}(0) = 0$ for SSM-INSAF
Parameters	$0 < \rho \leq 1$, $\gamma = \sqrt{t\sigma_{\eta}^2 / N}$, $\alpha = \left(\sum_{L=0}^{P-1} \rho^L \right)^{-1}$ $t \in [1, 4]$ for SM-INSAF $t \in [0.7, 0.9]$ for SSM-INSAF $\beta = 1 - N/\kappa M$, $\kappa \geq 1$ for SSM-INSAF
Adaptive process	$\bar{\mathbf{w}}(k) = \alpha \sum_{L=0}^{P-1} \rho^L \mathbf{w}(k-L)$ $\varepsilon_{i,D}(k) = d_{i,D}(k) - \mathbf{u}_i^T(k) \bar{\mathbf{w}}(k)$ $\mathbf{w}(k+1) = \bar{\mathbf{w}}(k) + \sum_{i=0}^{N-1} \frac{\mu_i(k) \varepsilon_{i,D}(k) \mathbf{u}_i(k)}{\ \mathbf{u}_i(k)\ ^2}$ <p>--SM-INSAF--</p> $\mu_i(k) = \begin{cases} 1 - \frac{\gamma}{ \varepsilon_{i,D}(k) }, & \text{if } \varepsilon_{i,D}(k) > \gamma \\ 0, & \text{otherwise} \end{cases}$ <p>--SSM-INSAF--</p> $\sigma_{\varepsilon_{i,D}}(k) = \beta \sigma_{\varepsilon_{i,D}}(k-1) + (1-\beta) \varepsilon_{i,D}(k) $ $\mu_i(k) = \begin{cases} 1 - \frac{\gamma}{\sigma_{\varepsilon_{i,D}}(k)}, & \text{if } \varepsilon_{i,D}(k) > \gamma \\ 0, & \text{otherwise} \end{cases}$

4 Simulation results

In order to evaluate the performances of both proposed SM-INSAF and SSM-INSAF algorithms, the Monte Carlo (MC) simulations (average of 30 independent runs) are performed in the contexts of system identification and acoustic echo cancellation. The unknown \mathbf{w}_o is a measured acoustic echo path with $M = 512$ taps (the sample rate is 8kHz). The cosine modulated filter bank with number of subbands $N = 8$ is used in all the SAF algorithms [2], unless otherwise specified. The system noise $\eta(n)$ is a white Gaussian signal with a low signal-to-noise ratio (SNR) of 10 or 5dB. Here, we

assume that the variance of the system noise, σ_η^2 , is known, because it can be easily estimated online in practice like in [3, 12, 19]. The normalized mean square deviation (NMSD), $10 \log_{10}(\|\mathbf{w}_o - \mathbf{w}(k)\|_2^2 / \|\mathbf{w}_o\|_2^2)$, (dB), is used as a measure of the algorithm performance.

4.1 System identification

In this section, the colored input signal $u(n)$ is generated by filtering a zero-mean white Gaussian signal through a first-order system $\phi(z) = 1/(1 - 0.95z^{-1})$ [20].

A) Effect of the parameters N , ρ , and P

We start by investigating one by one the effect of the parameters N , ρ , and P on the performances of the proposed algorithms. Here, the SNR is low, e.g., 10dB. Fig. 2 examines the convergence performance of the SM-INSAF algorithm using number of subbands $N=2$, 4, and 8. As expected, the algorithm with a large number of subbands (e.g., $N=8$) has faster convergence rate than that with a small one (e.g., $N=2$). The reason of yielding this phenomenon is that each subband input signal is closer to a white signal for a larger number of subbands. However, when number of subbands is larger than a certain value (in this case, $N=4$), this phenomenon will become weak.

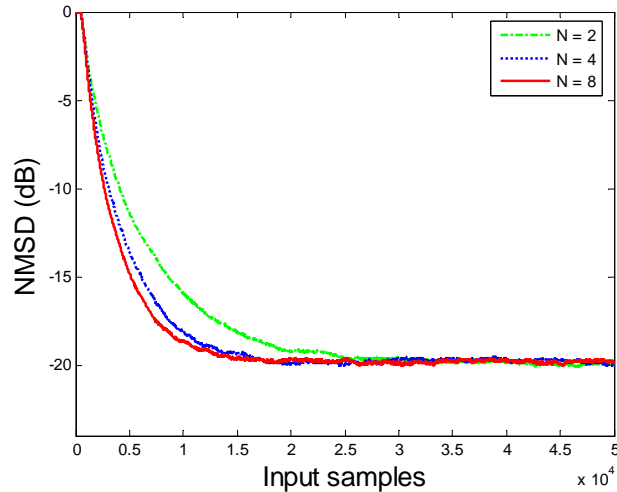


Fig. 2. The NMSD curves of the SM-INSAF algorithm using different number of subbands N . Other parameters: $P=3$, $\rho=1$, and $t=2$

Fig. 3 provides the NMSD results of the SM-INSAF algorithm using $\rho=0.2$, 0.6, and 1. As can be seen, the value of ρ is closer to 1, the steady-state performance is better while the convergence rate is slightly slow. Fig. 4 shows the NMSD results of the SM-INSAF algorithm using $P=1$, 2, and 3. Clearly, a higher number of using past tap-weight vectors (i.e., $P=3$) reduce the steady-state NMSD of the SM-

INSAF, whilst maintains almost the same convergence performance as the SM-NSAF (i.e., the SM-INSAF with $P=1$). Without loss of generality, the above results obtained from Figs. 2-4 are also reasonable for the SSM-INSAF algorithm, because both proposed algorithms use the same way to update the tap-weight vector, i.e., (20).

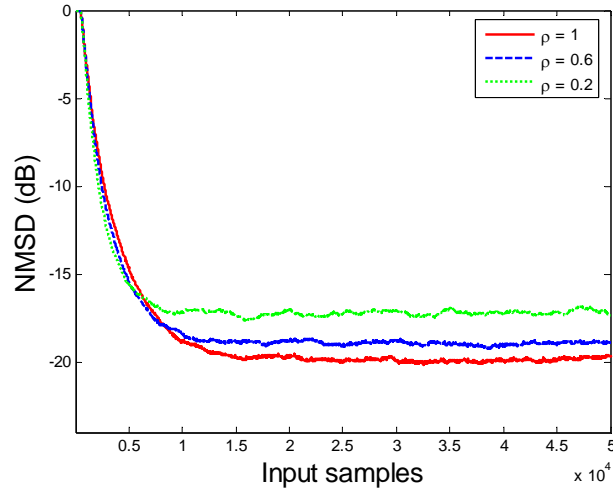


Fig. 3. The NMSD curves of the SM-INSAF algorithm using different values of ρ . Other parameters: $P = 3$, $N = 8$ and $t = 2$.

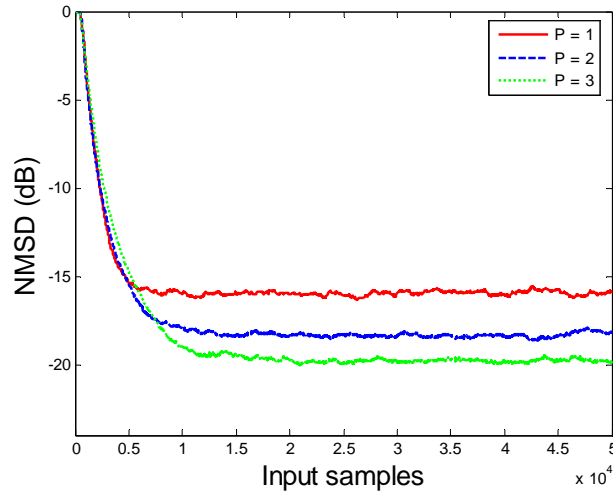


Fig. 4. The NMSD curves of the SM-INSAF algorithm using different values of P . Other parameters: $\rho = 1$, $N = 8$ and $t = 2$.

B) Performance comparisons

In this section, we compare both proposed algorithms with the NSAF, SM-NSAF [16] and INSAF [15] algorithms. To implement a fair comparison, we choose $N = 8$ for

all the SAF algorithms, $P=2$ for the INSAF, SM-INSAF and SSM-INSAF, and $\rho=1$ for the SM-INSAF and SSM-INSAF. Also, the tracking capabilities of the algorithms are checked by changing from \mathbf{w}_o to $-\mathbf{w}_o$ at the 5×10^4 th input sample.

Figs. 5 and 6 show the NMSD results of these algorithms in the case of SNR = 10 and 5dB, respectively. It is also concluded that both proposed algorithms are superior to the NSAF, SM-NSAF, and INSAF algorithms in terms of the convergence rate and tracking capability. As compared to the NSAF algorithm, the INSAF, SM-INSAF and SSM-INSAF algorithms work better in low SNR cases, since they use past tap-weight vectors in adaptation process. As one can also see, the SM filtering algorithms (e.g., the SM-NSAF, SM-INSAF and SSM-INSAF) achieve a good trade-off between the steady-state error and convergence rate in contrast to their counterparts (e.g., the NSAF and INSAF). This is due to the fact that these SM algorithms can also be considered as variable step size algorithms. Interestingly, both proposed algorithms (especially for the SSM-INSAF) provide better steady-state performance. In addition, it can be observed from Figs. 5 and 6 that the steady-state NMSDs of all the algorithms increase as the SNR decreases.

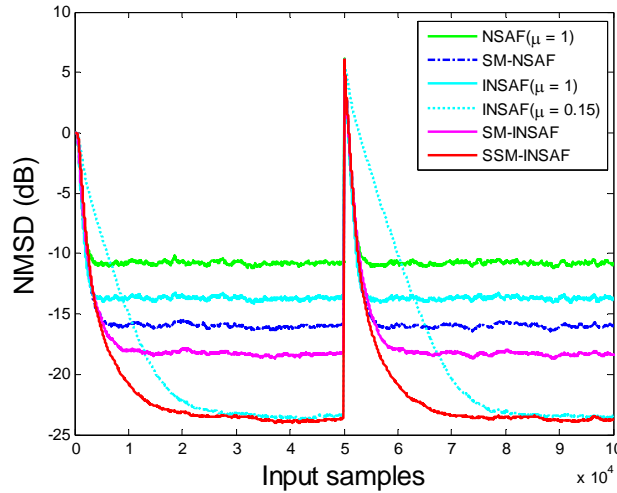


Fig. 5. The NMSD performance curves of various SAF algorithms in the case of SNR = 10 dB.

SM-NSAF: $\gamma = \sqrt{3\sigma_\eta^2 / N}$; SM-INSAF: $t = 2$; SSM-INSAF: $t = 0.75$, $\kappa = 1$.

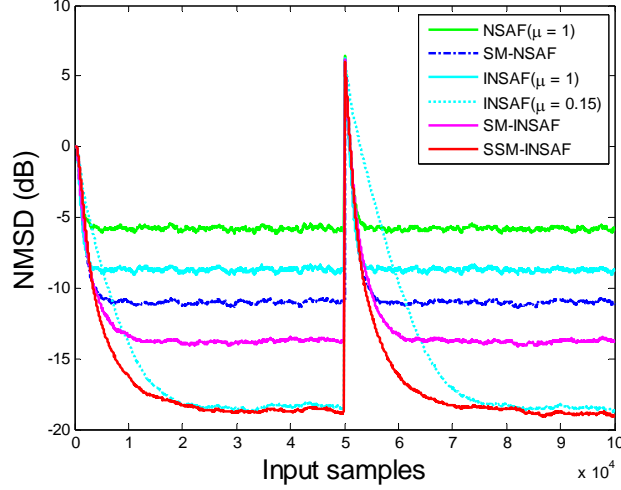


Fig. 6. The NMSD performance curves of various SAF algorithms in the case of SNR = 5 dB. Parameters' setting is the same as Fig. 5.

Table 2 gives a comparison of the above algorithms in the overall computational complexity by measuring the update rate (UR) for each subband, where the simulation condition is the same as Fig. 5. The URs for $i \in [0, N-1]$ are defined as $UR_i = (N_{update, i} / N_{total, i}) \times 100\%$, where $N_{update, i}$ and $N_{total, i}$ are the number of updates and the total number of iterations, respectively. As can be seen, all the SM filtering algorithms reduce significantly the overall computational complexity in comparison with the original NSAF and INSAF. Although the SSM-INSAF has larger UR_i than the SM-NSAF and SM-INSAF, it has the lowest steady-state error as shown in Fig. 5.

Table 2. The update ratio of each subband in various SAF algorithms for 125000 iterations

Algorithms	UR ₁	UR ₂	UR ₃	UR ₄	UR ₅	UR ₆	UR ₇	UR ₈
NSAF, INSAF	100%	100%	100%	100%	100%	100%	100%	100%
SM-NSAF	40.6%	33.8%	31.5%	31.3%	31.1%	30.9%	30.3%	29.8%
SM-INSAF	30.7%	26.5%	24.6%	24.1%	23.9%	23.7%	23.1%	22.2%
SSM-INSAF	53.4%	51.3%	50.3%	50.3%	49.9%	49.8%	49.5%	49.3%

4.2 Acoustic echo cancellation

Acoustic echo cancellation is a typical application of system identification [12, 19], i.e., identifying the acoustic echo path. The only difference is that the input signal is a true speech signal, as shown in Fig. 7. In this scenario, Fig. 8 plots the NMSD results

of these algorithms for SNR = 10 dB, wherein the change of the echo path from \mathbf{w}_o to $-\mathbf{w}_o$ occurs at the 1×10^5 th input sample. It is clear that both proposed algorithms still have better performances than other algorithms. In addition, the steady-state error of the SSM-INSAF is much smaller than that of the SM-INSAF.

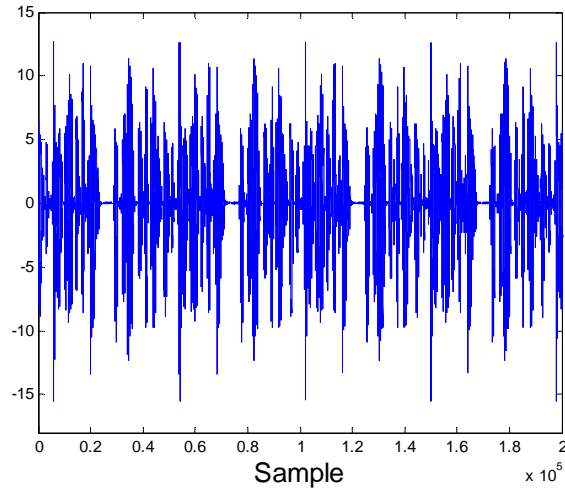


Fig. 7. Speech signal

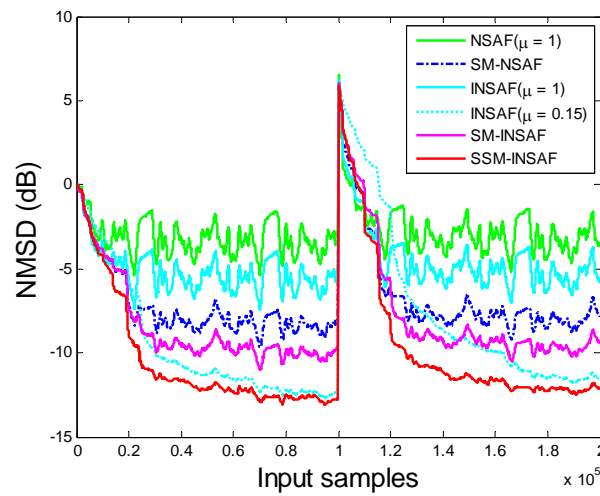


Fig. 8. The NMSD performance curves of various SAF algorithms for speech input. SNR = 10 dB. Parameters' setting is also the same as Fig. 5.

5 Conclusions

In this study, we derived the SM-INSAF algorithm by incorporating the concept of the SM filtering into the INSAF. Compared with the INSAF, the proposed algorithm not only provides better steady-state performance under the comparable convergence rate, but also saves the computational cost. Next, its smooth version, i.e., the SSM-INSAF, was proposed by smoothing subband error signals, thus further reducing the steady-state error. Simulation results have demonstrated that both proposed algorithms are superior to other existing algorithms in low SNR cases.

Acknowledgments

This work was partially supported by National Science Foundation of P.R. China (Grant: 61271340, 61134002, 61433011 and U1234203), the Sichuan Provincial Youth Science and Technology Fund (Grant: 2012JQ0046), the Fundamental Research Funds for the Central Universities (Grant: SWJTU12CX026).

Reference

1. A. Sayed, *Adaptive filters*. (New York, Wiley, 2008).
2. K. A. Lee, W. S. Gan, S. M. Kuo, *Subband adaptive filtering theory and implementation*. (Hoboken, NJ: Wiley, 2009).
3. Y. Yu, H. Zhao, An improved variable step-size NLMS algorithm based on a Versiera function. In Proc. IEEE International Conference on Signal Processing, Communication and Computing, pp. 1–4 (2013).
4. M. Z. A. Bhotto, A. Antoniou, A family of shrinkage adaptive filtering algorithms. *IEEE Trans. Signal Process.* 61(7), 1689–1697 (2013).
5. H. Cho, C. W. Lee, S. W. Kim, Deviation of a new normalized least mean squares algorithm with modified minimization criterion. *Signal Process.* 89(4), 692–695 (2009).
6. S. Gollamudi, S. Nagaraj, S. Kapoor, Y. F. Huang, Set-membership filtering and a set-membership normalized LMS algorithm with an adaptive step size. *IEEE Signal Processing Lett.* 5, 111–114 (1998).
7. S. Werner, P. S. R. Diniz, Set-membership affine projection algorithm. *IEEE Signal Process. Lett.* 8(8), 231–235 (2001).
8. Y. Yu, H. Zhao, B. Chen, Sparseness-controlled proportionate affine projection sign algorithms for acoustic echo cancellation. *Circuits, Systems, and Signal Process.* (2015). doi: 10.1007/s00034-015-0040-6
9. Y. Yu, H. Zhao, Memory proportionate APSA with individual activation factors for highly sparse system identification in impulsive noise environment. *IEEE Int. Conf. on Wireless Communications and Signal Process (WCSP)*, pp. 1–6 (2014).
10. K. A. Lee, W. S. Gan, On the subband orthogonality of cosine modulated filter banks. *IEEE Trans. Circuits Syst. II.* 53(8), 677–681 (2006).
11. K. A. Lee, W. S. Gan, Improving convergence of the NLMS algorithm using constrained subband updates. *IEEE Signal Process. Lett.* 11(9), 736–739 (2004).

12. Y. Yu, H. Zhao, B. Chen, A new normalized subband adaptive filter algorithm with individual variable step sizes. *Circuits, Systems, and Signal Process.* (2015). doi: 10.1007/s00034-015-0112-7
13. J. H. Seo, P. G. Park, Variable individual step-size subband adaptive filtering algorithm. *Electron. Lett.* 50(3), 177–178 (2014).
14. Y. S. Choi, S. E. Kim, W. J. Song, Noise-robust normalised subband adaptive filtering. *Electron. Lett.* 48(8), 432-434, (2012).
15. J. Ni, Improved normalised subband adaptive filter. *Electron. Lett.* 48(6), 320–321 (2012).
16. M. S. E. Abadi, J. H. Husøy, Selective partial update and set-membership subband adaptive filters. *Signal Process.* 88(10), 2463–2471 (2008).
17. M. S. E. Abadi, Selective partial update and set-membership improved proportionate normalized subband adaptive filter algorithms. *Int. J. Adapt. Control Signal Process.* 24, 786–804 (2010).
18. M. S. E. Abadi, S. Kadkhodazadeh, A family of proportionate normalized subband adaptive filter algorithms. *Journal of the Franklin Institute.* 348, 212–238 (2011).
19. C. Paleologu, S. Ciochin ă, J. Benesty, Variable step-size NLMS algorithm for under-modeling acoustic echo cancellation. *IEEE Signal Process. Lett.* 15 5–8 (2008).
20. J. W. Shin, N. W. Kong, P. G. Park, Normalised subband adaptive filter with variable step size. *Electron. Lett.* 48(4), 204–206 (2012).